Acid catalyst influence on the polymerization time of polyfurfuryl alcohol and on the porosity of monolithic vitreous carbon

Fábio Dondeo Origo,[1] Júlia Cassiano Arisseto,[1,2] Fernanda Lini Seixas,[3] Walter Miyakawa,[1] Alvaro José Damião,[1] Sílvia Sizuka Oishi,[4] Edson Cocchieri Botelho[4]

[1]Trevo Coronel Aviador José Alberto Albano do Amarante, Photonics Division, Institute for Advanced Studies/DCTA, 1, São José dos Campos, SP, CEP 12228-001, Brazil
[2]Federal University of São Paulo, R. Talim, 330, São José dos Campos, SP, CEP 12231-280, Brazil
[3]Chemical Engineering Department, Maringá State University, Maringá, Av. Colombo, 5790, PR, 87020-900, Brazil
[4]Materials and Technology Department, São Paulo State University - UNESP, Av. Ariberto Pereira da Cunha, 333, Guaratinguetá, SP, CEP 12516-410, Brazil
Correspondence to: F. D. Origo (E-mail: dondeo@ieav.cta.br)

ABSTRACT: This study compares the influence of different acid catalysts on the polymerization rate of polyfurfuryl alcohol (PFA) precursor and especially on the respective porosity of Monolithic Vitreous Carbon (MVC) produced from that. Five acid catalysts commonly used were compared: *p*-toluenesulfonic (PTLS), hydrochloric, sulfuric, nitric, and phosphoric. A fixed molar concentration of catalyst was diluted in PFA resin under room pressure and temperature. The time dependence of PFA resin polymerization was investigated by optical transmittance of PFA films, and the polymerization degree, characterized by ATR spectroscopy and thermogravimetry. MVC samples prepared with the same PFA resin and each catalyst were carbonized up to 1200 °C, under inert atmosphere. MVC porosity was studied by nitrogen adsorption/desorption, and by SEM and optical microscopy. Higher polymerization degree and higher residual mass were obtained with faster catalysts. No direct relation between the polymerization rate and the acid force was observed. PTLS promoted the fastest PFA polymerization process and the sulfuric acid, the slowest one. MVC samples were obtained by slow carbonization. MVC presented low specific surface S_{BET} from 1.4 to 7.4 m^2/g. Nitric acid catalyst contributed the most to micropores formation. Micrometric apparent porosity was smaller for the catalysts having longer polymerizations times, such as phosphoric and sulfuric acid. Phosphoric catalyst corresponded to the lowest porosity in MVC. As the polymerization time increased, the average size of the micrometric surface pores tended to augment. The MVC macroscopic porosity increased with the S_{BET} increment. Acid catalysts choice exerted a fundamental role on the porosity of MVC. © 2016 Wiley Periodicals, Inc. J. Appl. Polym. Sci. **2016**, *133*, 43272.

INTRODUCTION

Different carbonaceous materials can be obtained from polyfurfuryl alcohol (PFA) resin carbonization or pyrolysis. The products obtained by this processes range from selective membranes,[1] carbon microspheres,[2,3] hydrophobic surfaces,[4] activated nanoporous carbon,[5] carbon nanowires[6] to monolithic vitreous carbon[7] products. The Monolithic Vitreous Carbon material (MVC), which was studied in this article, is characterized by low density, good electrical conductivity, gas impermeability, resistance to high temperatures, biocompatibility, and chemical inertness.[8,9] Besides its well established use as high temperature crucibles, MVC has been proposed to novel applications such as microstructured molds,[10] substrate for nanoparticles[11] or graphene,[12]

electromagnetic radiation shield for atmospheric re-entry,[13] absolute intensity calibration standard for Small-Angle Scattering,[14] among many others.

MVC can only be obtained by very controlled heating process, when heating is slower than the shrinkage rate, to compensate the evolution of decomposition gases.[15] Pores are formed during the resin curing reaction and also during the carbonization process, when moisture and volatile gases are released.

Since 1950, acid-catalyzed resinification has been the most important industrial reaction of furfuryl alcohol.[16] The polymer formation rate is dependent upon the hydrogen ion concentration and the temperature, when furfural is polymerized by acids.[17] The

chemistry of furfuryl alcohol polymerization is initiated by heat, acids, and aluminas and it has proven to be complex.[16] The liquid resins have linear structures formed by intermolecular dehydrations of the hydroxyl group of one molecule, and the active α-hydrogen of another. When the resinification is stopped, at an intermediate fluid stage, with addition of a base, the resin can be stored for extended periods.[18] Also, according to Schmitt et al.,[18] the polyfurfuryl alcohol resin curing rate is largely dependent upon temperature, activity and acid catalyst concentration. A strong mineral acid generally results in a very rapid cure, while a complete cure is difficult when using weak acids.

Different acid catalysts can be used for the curing of PFA leading to the formation of different structures and morphologies after carbonization. According to Cheng and Tseng,[19] the use of acid for the polymerization of furfuryl alcohol (FA) produces a more ordered structure, when compared to a carbon obtained without acid, though with higher porosity.

Hucke[20] patented the production of porous carbonaceous materials by blending a carbon binder, a pore forming and a dispersant. That patent referred to materials with high porosity and interconnected pores, which is not the case of MVC, and also, with densities significantly lower than that of the MVC. This study is focused on the cure and posterior carbonization of the PFA resin using acid catalysts, and not on the well-studied process of resinification of FA. In spite of the numerous patents and papers already published regarding PFA products and MVC, there are still some interesting issues left to be studied: (1) how significantly can the catalyst choice affect the MVC porosity; (2) how does this porosity relate to the polymerization time of the precursor PFA and, finally: (3) at the same polymerization temperature, is the PFA polymerization rate dependent on the acid force? In this work, our major objective is to answer the above mentioned questions comparing five common acid catalysts under exactly the same conditions of polymerization/cure/carbonization, each one leading to a different polymerization rate. The catalysts compared were: p-toluenesulfonic (PTLS), hydrochloric, sulfuric, nitric, and phosphoric. This work is not meant to establish the exact cure mechanism, which is known to be extremely complex, but to provide quantitative data to help catalyst choice in PFA resin cure and MVC preparation. This experimental study is especially useful for the development of carbon materials with reduced micropore content, since porosity affects their mechanical properties and surface quality.

EXPERIMENTAL

Materials
Monolithic Vitreous Carbon samples were obtained from polyfurfuryl alcohol resin polymerization and carbonization. The resin presented 1.5% (w/w) moisture, viscosity of 711 mPa s and pH 7.5 (neutralized). Those values correspond to low macroscopic porosity samples of polymerized PFA, as described in our previous work.[21] The acid catalysts commonly applied for furfuryl alcohol polymerization[19] were also employed in this study: p-toluenesulfonic monohydrate (PTLS), hydrochloric, sulfuric, nitric, and phosphoric. All the commercial P. A. catalysts were diluted in distilled water, so that a final concentration of 30% (w/w) could be reached, considering the initial water

percentage of the commercial acids. In order to make the comparison of catalysts effects more effective, another constraint was adopted in this study: the use of a fixed ratio R of 10^{-4} moles of catalyst per gram of PFA resin for each catalyst solution. This value was chosen based on previous tests to achieve the typical concentration necessary to polymerize polyfurfuryl alcohol, with the use of different catalysts. Each catalyst solution was added to the resin to obtain the intended ratio R. The polyfurfuryl alcohol resin was mixed with each catalyst solution and homogenized for five minutes. Afterwards, the mixture was centrifuged at 3000 rpm for 3 min, to reduce the presence of air bubbles, which appear due to the catalyst addition and also to the polymerization reaction starting. Finally, the resin was poured into clean silicone rubber molds to produce cylindrical samples with 25 mm in diameter, and a thickness of 9 mm.

PFA Optical Transmittance
A Jasco V570 spectrophotometer (300 − 2000 nm) was employed to measure the optical transmittance variation during the cure of the PFA resin. The purpose was to compare the polymerization rate, for each catalyst studied, by measuring the time evolution of the resin thin film transmittance at a fixed wavelength of 1500 nm (T_{1500}). This wavelength was chosen because the PFA transmittance is relatively higher in this range of the spectrum.

A few drops of the centrifuged resin, prepared as described before, were poured in the center of a transparent glass microscope slide. The total mass of added resin was measured to assure that the same amount of mass was used for each catalyst. At the borders of that slide, a double-sided tape was previously fixed. Another glass slide was pressed against the prior slide that contained the resin, gently spreading it, in order to form a resin film between them, with a thickness of 75 (± 10) μm. That value corresponded to the thickness of the double-sided tape used as a separator between the two slides.

For the time scale, $t = 0$ s was the instant when the catalyst was added to the resin. The first measurement was done at $t = 15$ min. The transmittance measurements for each film were repeated initially at 15-min intervals, then, the measurement intervals were increased to hours, then to days, according to the transmittance variation. All the transmittance measurements were performed at room temperature. The curve of T_{1500} as a function of time was normalized to the transmittance value of the first measurement, at $t = 15$ min. Transmittance normalization was also employed in Ref. 22 to allow better comparison of different samples of FA polymerization.

Characterization of Polymerized PFA Resins
Attenuated Total Reflection (ATR-IR) spectra were measured using a Shimadzu IR Affinity-1 spectrophotometer. Measurements were carried out one month after the addition of each catalyst, for the polymerized PFA resins, at room temperature, without thermal curing.

Thermogravimetric analyses of noncured samples were performed with a SII Nanotechnology Exstar TGA/DTA 6200 (Seiko Instruments Inc.), from ambient temperature to 1000 °C, with a constant 10 °C/min heating rate, in nitrogen flow environment.
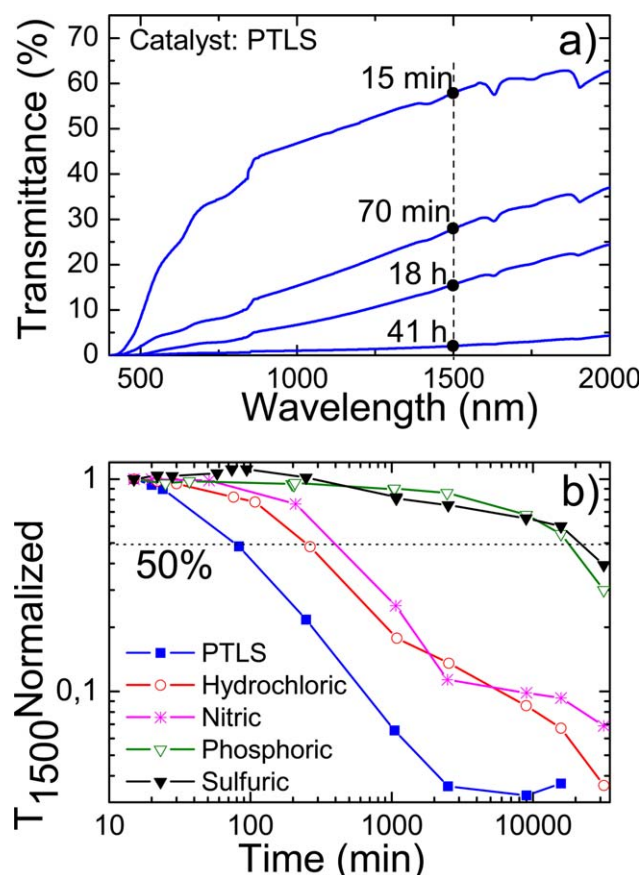
Figure 1. (a) Optical transmittance evolution of polyfurfuryl alcohol catalyzed with PTLS. The vertical line represents transmittance at 1500 nm; (b) Normalized optical transmittance, at 1500 nm, as a function of time for different acid catalysts. Horizontal dashed line corresponds to a 50% reduction in transmittance. [Color figure can be viewed in the online issue, which is available at wileyonlinelibrary.com.]

Cure and Carbonization

The cylindrical samples were left for 1 month at room temperature after preparation, to ensure their polymerization. They were, then, post-cured at 100 °C for 30 min in ambient atmosphere and demolded. Carbonization was carried out in a tubular furnace (EDG FT-HI), with N_2 atmosphere, at low heating rates: 0.2 °C/min from room temperature to 100 °C; reduced to 0.1 °C/min from 100 °C to 600 °C, when most volatiles leave the matrix; 0.2 °C/min from 600 °C to 1200 °C. After 2 h at 1200 °C, the temperature was decreased at 0.75 °C/min rate to room temperature.

Specific Surface Area

For each catalyst, a cylindrical MVC sample was milled (nearly 0.5 g) and analyzed by conventional nitrogen adsorption isotherm at −196 °C, with the use of a Quantachrome NOVA-1200. Before measuring, the powder was degassed at 300 °C for 12 h. The results were analyzed with the software NovaWin. The specific surface areas S_{BET} were estimated by the BET[23] method. The Dubinin-Radushkevich method[24] was employed to estimate the micropore volume.

Surface Porosity

The MVC samples were polished with diamond powder and cleaned by ultrasonication with acetone and isopropyl alcohol. After cleaning, they were characterized by optical microscopy using a BX51 Olympus microscope, in reflection mode. Ten micrographs, of different regions, were taken for each polished surface, using 200X magnification. From these data, the average of area fraction covered by pores, and the area of each single pore, were calculated using the free software ImageJ. Here, apparent porosity refers to the fraction of surface covered by pores, designated as P_{TOTAL}. The darker regions correspond to pores (valleys), as verified with a high precision profiler (Taylor Robson PGI 1000).

The smallest micrometric structures were observed by scanning electron microscopy (Hitachi TM3000), with 3000X magnification. Before that, a Cu thin film was deposited on the samples to reduce charging effects. The scanned images were obtained through collections of backscattered electrons under 15 kV accelerating voltage. At least four different regions were observed for each surface studied, for a given magnification.

RESULTS AND DISCUSSION

Polymerization

The color of PFA resin films changed from light yellow to dark brown along the polymerization process. In Figure 1(a), the film transmittance evolution corresponding to PTLS catalyst is shown as a typical example. The vertical dashed line detaches the transmittance variation at 1500 nm. Figure 1(b) displays the normalized transmittances at 1500 nm (T_{1500}) plotted as a function of the time, extracted from the transmittance curves. The optical transmittance decreased as a function of the time, as the film became more opaque due to polymerization/curing process. The cure period using PTLS, hydrochloric and nitric acids was of one day, whereas for the other catalysts, the resin was cured only after some weeks.

All the $T_{1,500}$ curves decreased with time, except for sulfuric acid catalyst, which initially increased at 100 min, reached a maximum increment of 10% and then started to decrease as the other curves. This increase was related to micrometric bubbles formation, which could be observed by optical microscopy. The bubbles increased the respective film transparency, more pronouncedly for this catalyst. To quantify the polymerization rate for each catalyst, the time $t_{50\%}$ corresponding to a 50% reduction in transmittance (horizontal dotted line) was compared in Table I, as the dissociation constant pKa[25] for each acid catalyst. All the log−log curves presented a linear region inside the

Table I. pKa (dissociation constant),[25] $t_{50\%}$, γ, and C for each catalyst

Catalyst	pKa	$t_{50\%}$ (min)	γ	C (min)
PTLS	−2.8	78	0.775	33.0
Hydrochloric	−7	250	0.579	69.8
Nitric	−1.3	485	0.758	153.0
Phosphoric	+2.1	17866	0.031	30.6
Sulfuric	−2.8	21445	0.119	220.6

interval which ranges from 100 min to 2500 min. Therefore, the transmittance decrease was represented by the Equation (1), which corresponds to a simple linear function in this scale:

$$\bar{T}_{1,500} = (C/t)^{\gamma} \qquad (1)$$

Where C and γ are constants for each catalyst, and $t (>0)$ is the time ($t = 0$ s corresponds to catalyst addition). The higher the γ value, the faster the transmittance curve decreases and, consequently, the greater the polymerization rate is. The γ and C values are also shown in Table I. All the linear fittings corresponded to a linear regression coefficient above 0.96.

The linear trend is different from that observed in furfuryl alcohol polymerization,[22] which presented a linear behavior in linear-log scale when the transmission through a volume of resin was studied. Possibly, they behaved differently due to the bidimensional nature of the film and especially due to the fact that the polymerization rate is different in furfuryl alcohol (FA) and in polyfurfuryl alcohol resin (PFA). In addition, two different groups of catalysts were identified: (1) PTLS, hydrochloric, and nitric acids that corresponded to fast polymerization, with $t_{50\%}$ in hours; (2) phosphoric and sulfuric acids, with slow polymerization and $t_{50\%}$ in weeks. The angular coefficient γ, from Table I, presented the trend of increasing as $t_{50\%}$ increased, so, any of those two parameters could be used to evaluate the polymerization rate from the transmittance curve of the resin. The polymerization results on Table I did not present direct relation with the dissociation constant pKa of each catalyst. According to Schmitt et al.,[18] the cure rate of polyfurfuryl alcohol resin is largely dependent upon temperature, activity, and concentration of the acid catalyst. A strong mineral acid generally results in a very rapid cure, while a complete cure is difficult when using weak acids. In our work, with the same room temperature and concentration for all catalysts, only the catalyst activity was different. Therefore, in this experiment, cure rate was not proportional to its catalyst acid activity. For instance, sulfuric acid catalyst was one of the strongest acids employed in this study; however, its polymerization rate was very slow, similar to that of the weak phosphoric acid.

Sulfuric acid is very reactive with FA[26] and frequently employed as FA catalyst.[18,19] However, in the concentrations of this study, sulfuric acid could not be efficiently dissolved and homogenized in the PFA resin. With the FA polymerization progression, the number of hydroxyl groups per gram of initial monomer material decreases.[18] FA is highly soluble in water,[18] but PFA resins are only partially soluble in water,[22] indicating low polarity of PFA resin.

In a simple manner, solubility of a substance is related with the polarity, which is in turn associated with the dielectric constant. Water is highly polar and presents a dielectric constant of 80,1.[27] The dielectric constants of the pure inorganic acids employed as catalysts are: 106 for sulfuric acid,[28] 61 for phosphoric acid,[28] 50 for nitric acid,[29] and 14 for hydrochloric acid.[30] As the organic solvent (PFA resin) is non-polar, the lower the catalyst dielectric constant, the higher should be its solubility in PFA. In our experiments, polymerization times
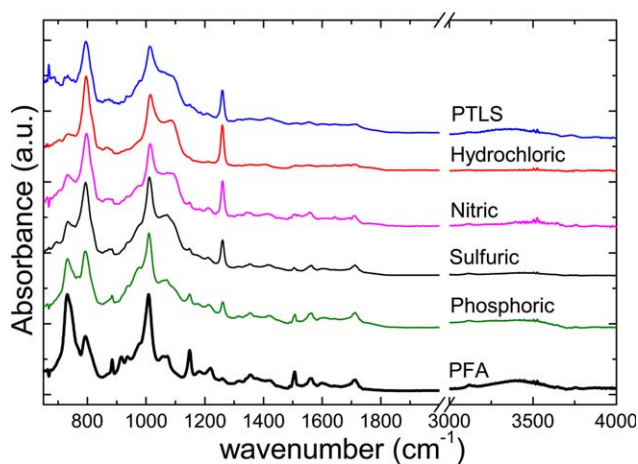

Figure 2. FTIR spectra from PFA resin and PFA polymerized with each acid. [Color figure can be viewed in the online issue, which is available at wileyonlinelibrary.com.]

have indeed decreased with the catalyst dielectric constants. The PTLS acid was the fastest catalyst due to the presence of an organic part, which helped its dissolution in PFA (organic solvent). Hence, it can be concluded that the polymerization degree of a catalyst depends on its solubility in the catalyzed substance—PFA resin, in our case. And this is the reason no direct relation was observed between the catalyst pKa and the corresponding polymerization time.

Polymerized PFA Characterization

Figure 2 shows the ATR-IR spectra of the nonpolymerized PFA, and the polymerized PFA resins with different catalysts after one month, at room temperature. Some important bands were modified by the polymerization process. Bands centered at 728 cm^{-1}, and at 880 cm^{-1}, assigned to the hydrogen of furan ring, have decreased. Reduction in vibrational bands of the furan ring[31] assigned to the $=C-O-C=$ stretching at 1016 cm^{-1}, the $-C=C-$ at 1500 cm^{-1} and the C$-$O at 1146 cm^{-1}, and to the OH$^-$ stretching at 3400 cm^{-1}[31] were also observed. Increase in band intensities could be seen at 795 cm^{-1}, the characteristic 2.5-disubstituted furan ring, and at 1260 cm^{-1} assigned to the asymmetric and symmetric stretching vibrations of the $=C-O-C$ groups from 2-substituted furan ring.[21,31]

The polymerization degree can be evaluated by calculating the diagnostic band shape parameter α, as proposed by Barsberg and Thygesen.[32] According to them, the smaller the quotient between intensities (I), or areas of the decomposed bands, $I_{728} + I_{750}$ by ($I_{782} + I_{790} + I_{803}$), the farther is the reaction progress, and hence, the higher is the polymerization degree. The decomposed bands at 728, 750, 782, 790, and 803 cm^{-1}, were determined by spectra deconvolution in the interval $700 - 850$ cm^{-1}, using Lorentzian functions, as represented in Figure 3. Clearly, PFA band intensity predominance changes from 728 cm^{-1} to 795 cm^{-1}. In Table II, calculated α values for the nonpolymerized and the polymerized PFA resins are shown. It can be concluded that the PFA resin polymerization degree decreases in the order PTLS acid > hydrochloric acid > nitric acid > sulfuric acid > phosphoric acid.
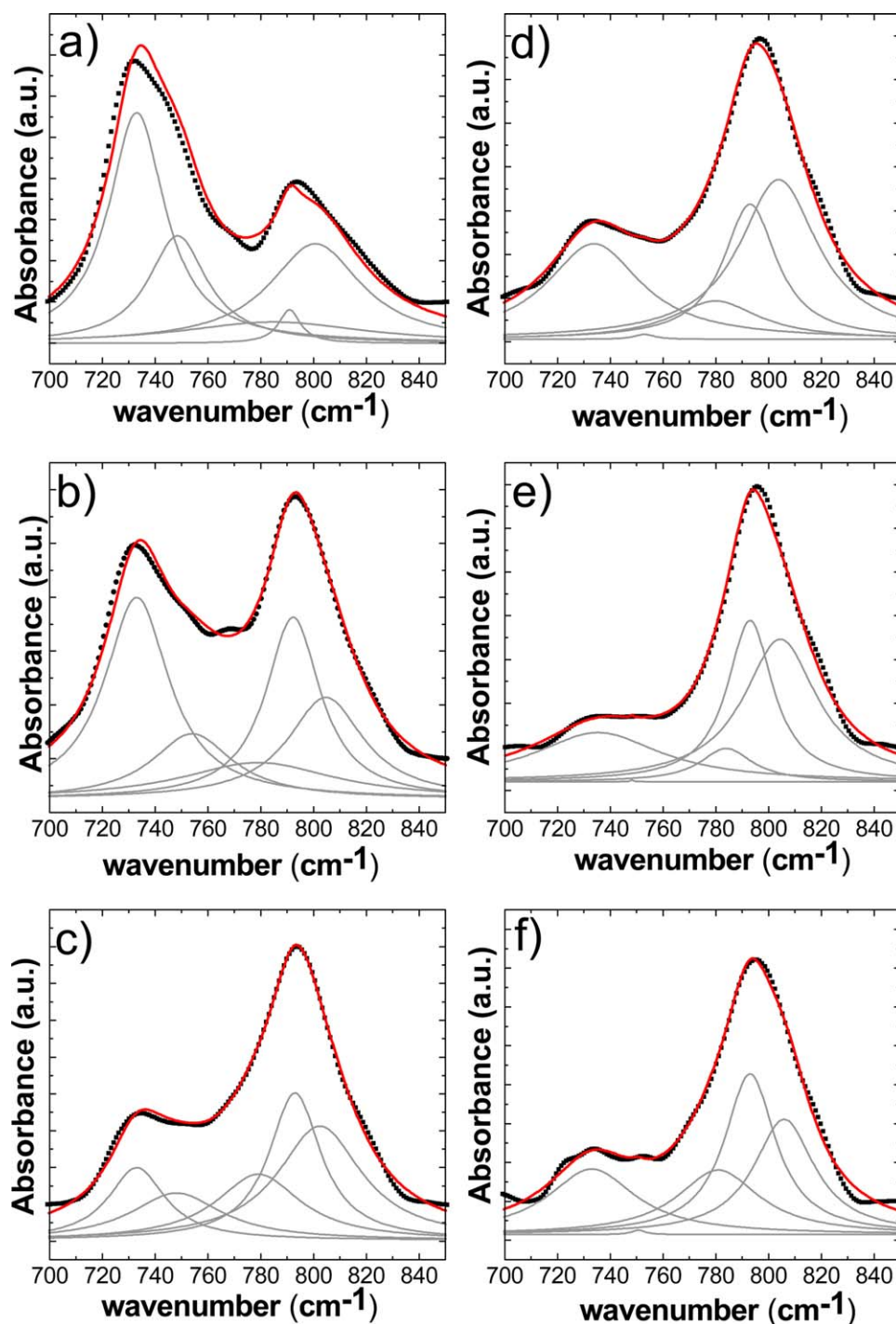
Figure 3. Absorbance from FTIR spectra. Black squared curves correspond to experimental measurements. Gray curves correspond to the best fitting using Lorentzian curves. Thick red line is the sum of the five Lorentzian curves; (a) PFA pure resin; PFA resin polymerized with: (b) phosphoric acid, (c) sulfuric acid, (d) nitric acid, (e) hydrochloric acid, and (f) PTLS acid. [Color figure can be viewed in the online issue, which is available at wileyonlinelibrary.com.]

Table II. Estimative of the degree of polymerization from infrared bands in the 750 cm^{-1} to 800 cm^{-1} region

Material	PFA resin	PFA/H$_3$PO$_4$	PFA/H$_2$SO$_4$	PFA/HNO$_3$	PFA/HCl	PFA/PTLS
Degree of polymerization	1.54	0.80	0.36	0.36	0.26	0.25

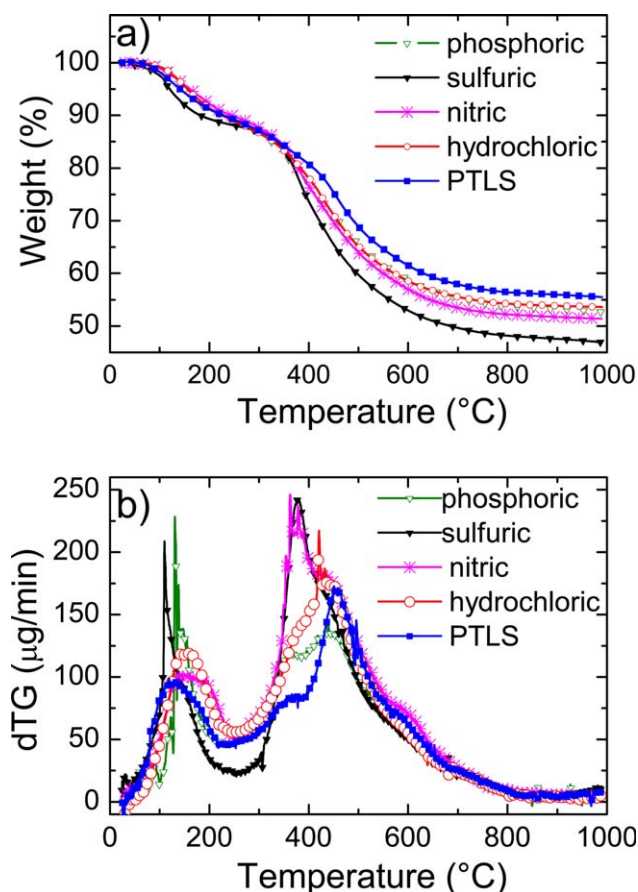Results for pure PFA resin, and uncured PFA resin, polymerized with each acid catalyst.

Figure 4. (a) Thermogravimetric analyses of polymerized PFA resin, for each acid; (b) Weight loss rate for each catalyst. [Color figure can be viewed in the online issue, which is available at wileyonlinelibrary.com.]

Thermal degradation of polymerized PFA resins was analyzed by thermogravimetry (TGA). Figure 4 shows TGA and respective first-derivative weight loss curves (DTG). The thermal decomposition temperature T_d (temperature at 10% weight loss), and residual weight at 1000 °C data were presented in Table III.

T_d varied from 181.6 °C to 262.8 °C, and residual weight, from 46.9% to 55.5%. The sulfuric acid catalyzed PFA presented the lowest thermal stability and residual weight, and consistent low polymerization degree as well. DTG curves showed similar weight loss for sulfuric and phosphoric acid between 50 °C and 250 °C, due to the presence of volatiles and low molecular weight compounds. Dehydration primarily occurs between 30 °C and 200 °C. Weight loss between 300 °C and 700 °C is, in turn,

Table III. Thermal decomposition temperature (T_d) and residual weights (at 1000 °C) of uncured PFA resin, polymerized with each catalyst

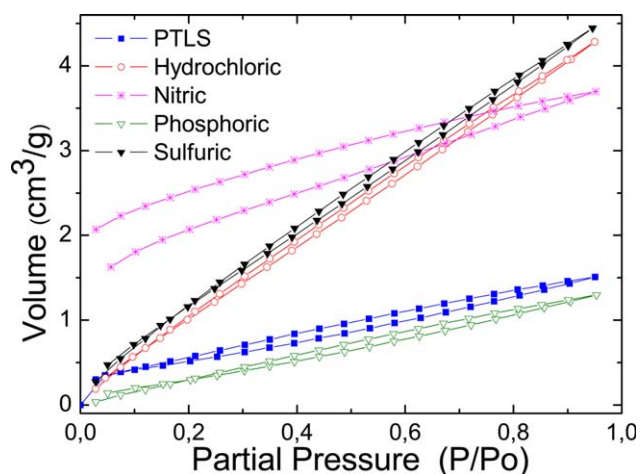|	PTLS	HCl	HNO$_3$	H$_3$PO$_4$	H$_2$SO$_4$
T_d (°C)	228.3	225.6	244.2	230.0	181.7
Residual weight (%)	55.5	53.6	51.4	52.6	46.9

Figure 5. Nitrogen adsorption/desorption isotherms for MVC produced with different catalysts. [Color figure can be viewed in the online issue, which is available at wileyonlinelibrary.com.]

generally attributed to the release of CO, CO$_2$, CH$_4$, H$_2$O, and H$_2$.[9] However, in spite of the worst polymerization degree, the phosphoric acid catalyzed PFA has evidenced better thermal stability and higher residual weight compared with the sulfuric acid. The PTLS and HCl catalysts yielded best polymerization degree, low volatility, higher residual weight and good thermal stability. From DTG curves, it can be concluded that different acid catalysts have different degradation mechanisms.

Carbonized MVC sample diameters were also measured comparatively to the initial size of polymerized PFA resin, before the carbonization. After carbonization, sample diameters were 78($\pm$2)% of the initial size, showing no dependence on the catalysts.

Surface Specific Area

Figure 5 shows the isotherms of N$_2$ adsorption and desorption of MVC samples for each catalyst. The results can be classified in three different groups: (1) PTLS and phosphoric acid, corresponding to lower gas adsorption; (2) hydrochloric and sulfuric acids related to intermediate adsorption; (3) nitric acid catalyst, which promoted larger hysteresis than the other catalysts.

Table IV shows the specific surface area calculated by multi-point BET method. Micropore volume was calculated using the Dubinin-Radushkevich (DR) method. Specific micropore volume whose values were lower than 4.10^{-3} cm^3/g did not allow reliable pore distribution calculations.

Table IV. Specific surface area (S_{BET}) and micropores volume (V_{mic})

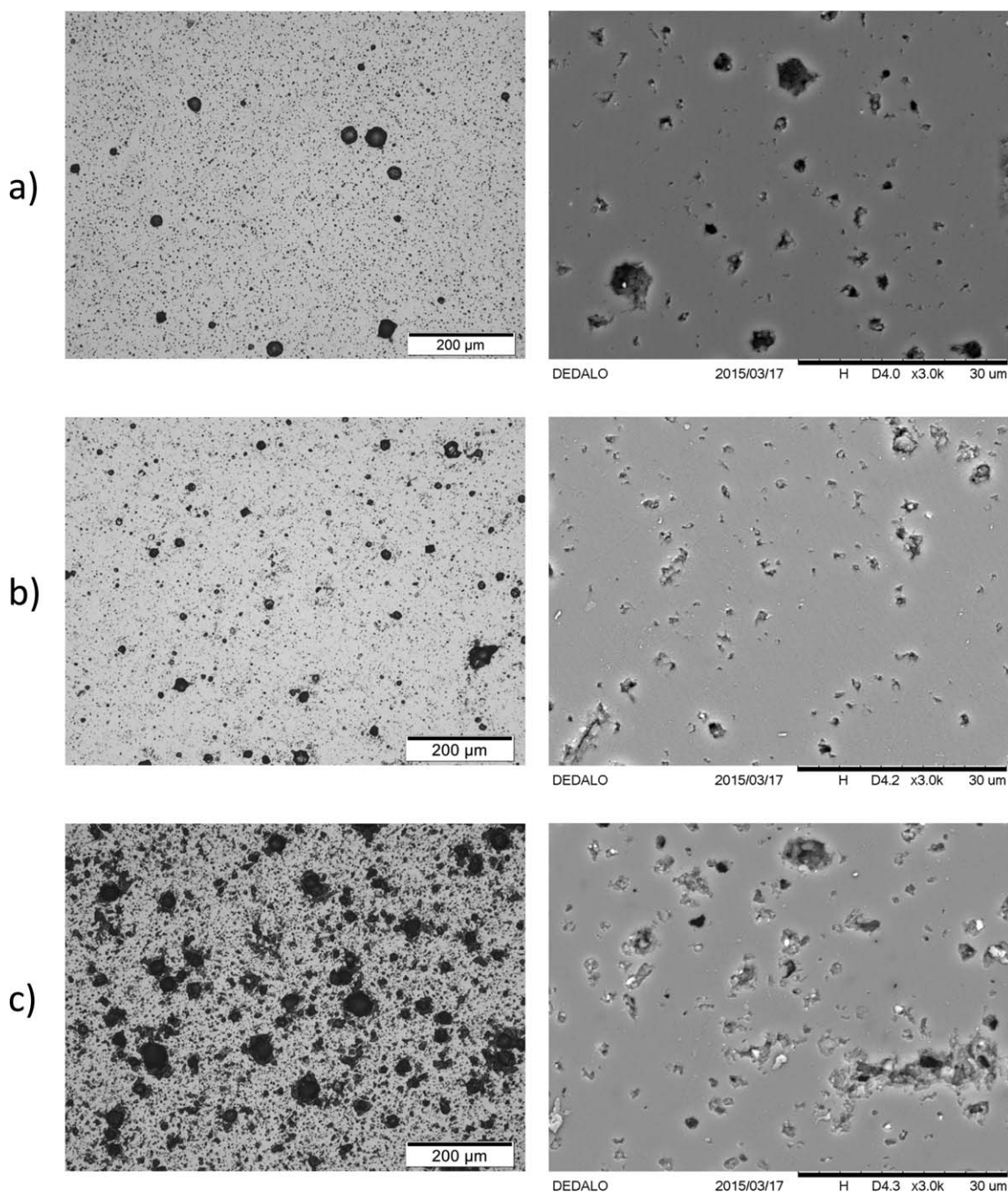| Catalyst	S_{BET} (m^2/g)	V_{mic} (cm^3/g)
PTLS	2.0 ($\pm$0.1)	1.10^{-3}
Hydrochloric	5.9 ($\pm$0.3)	2.10^{-3}
Nitric	7.4 ($\pm$0.4)	4.10^{-3}
Phosphoric	1.4 ($\pm$0.1)	$<1.10^{-3}$
Sulfuric	5.7 ($\pm$0.3)	2.10^{-3}

Figure 6. (a) Optical Microscopy (left column) and SEM (right column) for each acid catalyst: (a) PTLS, (b) hydrochloric, (c) nitric, (d) phosforic, and (e) sulfuric.

Surface Micrometric Porosity

Figure 6 displays optical and SEM micrographs for each catalyst: The PTLS acid, which corresponded to the fastest polymerization, presented the largest proportion of small pores. The MVC obtained with nitric acid has very large porosity, with both large and small pores. The sample cured with phosphoric acid presented the lowest porosity.

Due to the presence of two distinct classes of pores in the micrographies, the first one corresponding to pores with tens of micrometers, and the other class of a few micrometers, the pores were

arbitrarily classified into two distinct groups: larger micrometric pores, which present an area equal to or larger than 28.3 μm^2, the equivalent to a circle area with 3 μm radius, and small micrometric pores corresponding to pores with areas smaller than the ones of the larger micrometric pores. This limiting pore area, corresponding to a 3 μm radius, was chosen based on the pore distribution by size (not shown), obtained from the micrographies. P_{TOTAL} is the fraction covered by all the observed micrometric pores, independently of their sizes, in the optical micrographies. P_{LARGE} corresponds to the area fraction covered by the larger
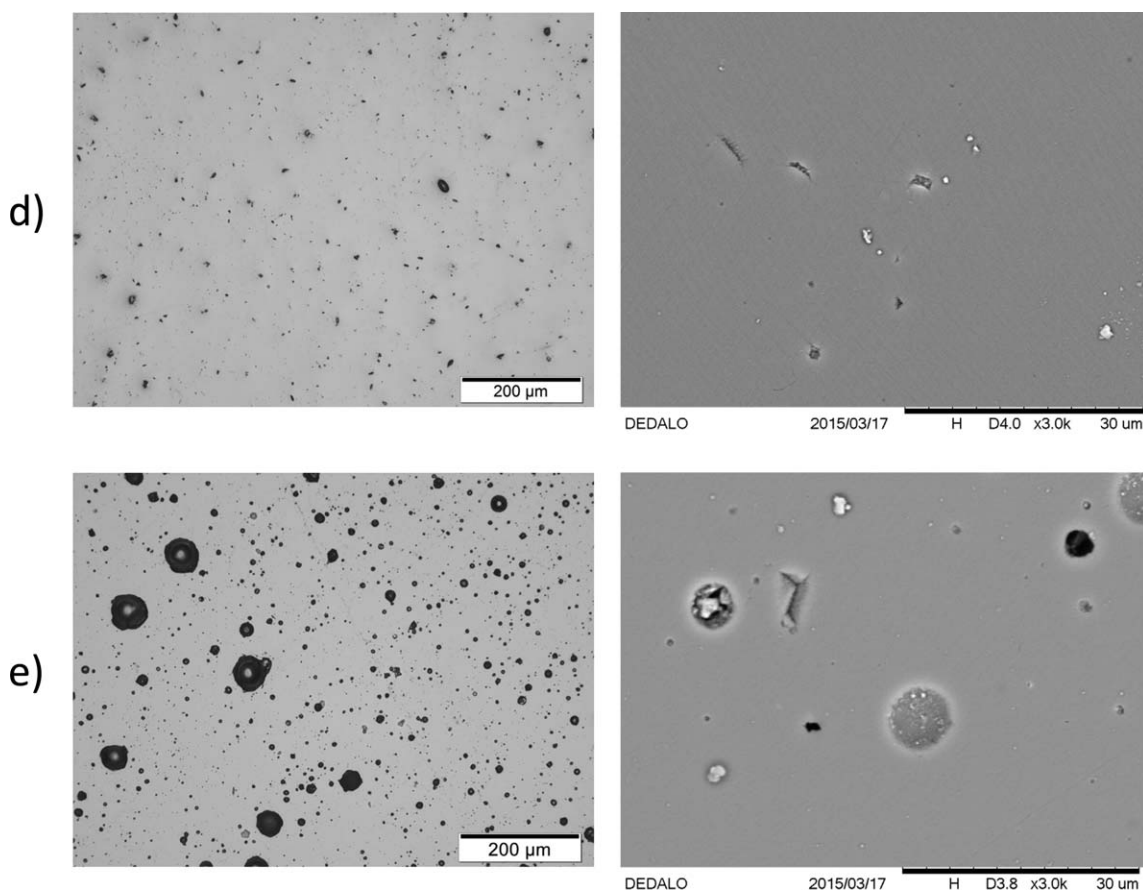
Figure 6. (Continued).

micrometric pores (area ≥ 28.3 μm^2) and P_{SMALL} is the area fraction covered by smaller pores (area < 28.3 μm^2). As shown in Figure 7(a), the micrometric pore area fraction P_{TOTAL} (sum of P_{SMALL} and P_{LARGE}) varied significantly from 3.7% to 22.7%, depending on the catalyst employed. The MVC samples produced with the catalysts with shorter $t_{50\%}$ presented larger porosity (P_{TOTAL}).

Figure 7(b) presents, for all the five catalysts, the ratio between the areas covered by small (P_{SMALL}) and large pores (P_{LARGE}) as a function of the respective $t_{50\%}$ (from Table I). It shows that the proportion of large micrometric pores (area ≥ 28.3 μm^2) increased as the polymerization time increased.

SEM data corresponding to each catalyst showed that the slowest catalysis—sulfuric and phosphoric acids—presented fewer pores and relatively small amount of small pores. That corroborates with the optical microscopy results. On the other hand, nitric, PTLS, and hydrochloric acids presented high surface density of small micrometric pores, with Feret diameter ratio below 3 μm. For all the catalysts, the density of submicrometric pores was negligible, as observed in SEM images (Figure 6) and confirmed at 10.000X magnification (not shown).

Microporosity may also be influenced by the maximum preparation temperature: during the pyrolysis of PFA, with a high heating rate of 10 °C/min, at 200 °C the matrix was essentially nonporous. According to IUPAC classification,[33] micropores correspond to pores of up to 2 nm, macropores are pores greater than 50 nm, and mesopores correspond to pores with sizes between micro and macro ranges. Micro and mesopores were originated at 300 °C and above 500 °C the mesopores start to collapse.[34] The S_{BET} of MVC reaches a maximum at 700 °C and is strongly reduced to ~ 5 m^2/g at 1100 °C (and higher temperatures).[35] This result was close to the specific surface areas S_{BET} obtained in this study, that were below 8 m^2/g. The adsorption/desorption curves showed in Figure 5, present Type-II shape, that is associated with high degree of nonporosity (or macroporosity). They have a similar shape of the adsorption isotherms of nonporous carbon coated silica.[36] The nitric acid curve is the only exception, and shows significantly higher hysteresis, which is associated to the capillary condensation in the mesopores. Its higher step at lower pressures is also an indicative of higher microporosity than the other MVC samples. That hysteresis shape, with adsorption/desorption curves meeting each other only close to the origin, was also found in micrometric particles of PFA carbonized at 600 °C.[19] Therefore, the MVC prepared with nitric acid presents the highest porosity, which is confirmed by its higher S_{BET} value. When comparing the MVC produced in this study with other materials, the S_{BET} is even lower than other nonporous ungraphitezed carbons, with values from 25 to 84 m^2/g.[37]
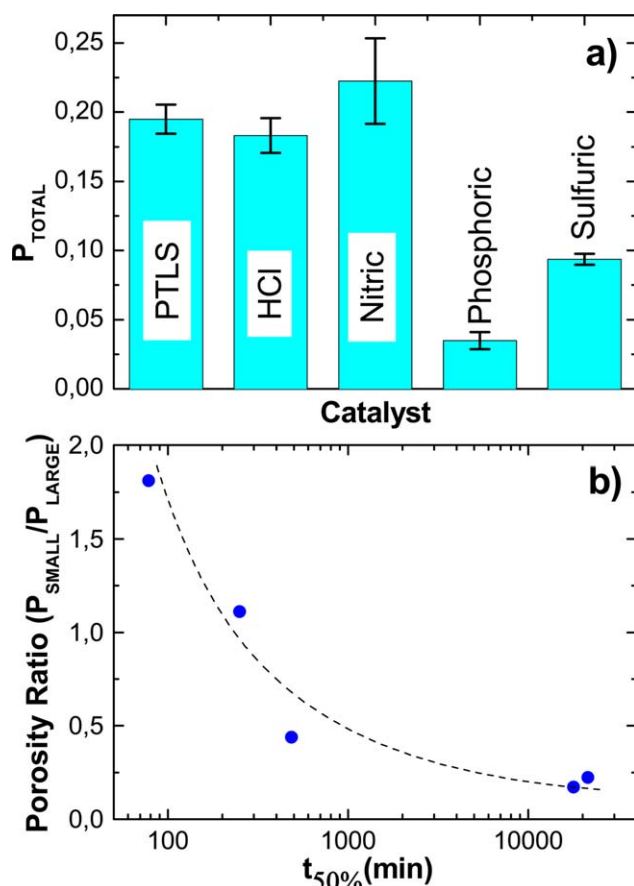
Figure 7. (a) Area fraction (P_{TOTAL}) occupied by all the micrometric pores. Vertical bars represent the standard deviation of the mean; (b) ratio between the surface area occupied by small pores P_{SMALL} (equiv. to radius ≤ 3 μm) and large pores P_{LARGE} (equiv. to radius >3 μm) as a function of $t_{50\%}$. The dashed curve is a guide to the eyes. [Color figure can be viewed in the online issue, which is available at wileyonlinelibrary.com.]

The low specific surface is coherent with the closed pore structure of MVC prepared at 1200 °C.[8] SAXS measurements of gyration radius of MVC pores prepared at 1200 °C varies from 1.3 to 1.4 nm,[38] and 2.5 nm.[35]

The catalysts that corresponded to slower polymerization also presented the lowest MVC porosity of micrometric pores. The range of MVC micrometric porosity measured in this study is of the same order of porosity found in similar PFA cured at 150 °C.[21] This macroporosity, formed by voids present in the hardened prepyrolysed polymer precursor was originated from decomposition products trapped beneath the rapidly pyrolyzed and densified surface layer.[36] As the polymerization time increases, the P_{SMALL}/P_{LARGE} ratio decreased. For instance, PTLS and Hydrochloric acids, with the shortest values of $t_{50\%}$ presented larger density of smaller micropores, as shown in SEM images. Therefore, longer times to polymerize, with slower increment in the resin viscosity, allow the coalescence of small pores to form larger pores. Depending on the application of the MVC pieces, it is possible to reduce the superficial area of micrometric pores by applying epoxy to close those large pores.[39]
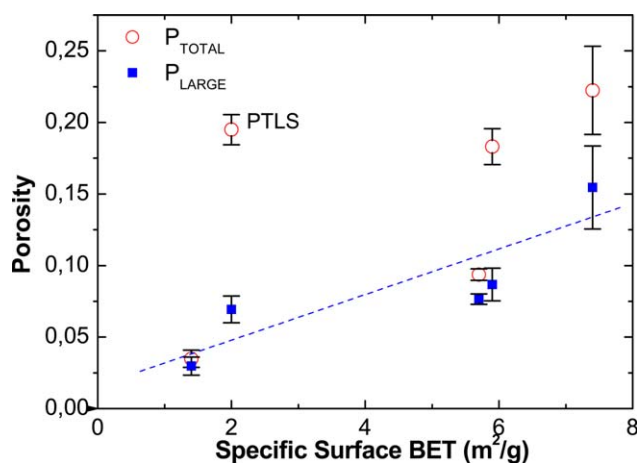

Figure 8. Relation of porosity obtained from Optical Microscopy with the specific surface S_{BET} from the adsorption/desorption curves of polyfurfuryl alcohol catalyzed after heat treatment with all the five catalysts from this study. Circles correspond to total porosity (P_{TOTAL}) and squares to the area covered by pores larger than 28.3 μm^2 (P_{LARGE}). The traced line is a guide to the eyes. [Color figure can be viewed in the online issue, which is available at wileyonlinelibrary.com.]

Finally, a correlation between the micrometric porosity and the measured surface S_{BET} was found for all the mineral acids studied, as shown in Figure 8. In general, when the S_{BET} area increases, the macroscopic porosity also increases, showing a relation between the nanometric and the macroscopic porosities. PTLS, which was the only organic acid used in this study, did not follow the same trend. It was the only catalyst whose fraction of small micrometric pores was much larger (64%) than the area occupied by larger micrometric pores. We believe that for the PTLS acid, before resin polymerization, the smaller pores formed close to the surface moved more easily toward the sample surface than the larger micrometric pores. As a consequence, the surface porosity obtained from microscopy was larger than the porosity value of the bulk, measured by gas adsorption. When representing only the contribution of larger pores (P_{LARGE}) against S_{BET} area, as show in Figure 8, a simple linear relation is observed. The increase in P_{LARGE} is related to an increase in S_{BET}. Since optical microscopy is simpler than the gas adsorption technique, we suggest this fast method to make relative S_{BET} comparisons among distinct MVC samples.

CONCLUSIONS

The polymerization rate at room temperature for polyfurfuryl alcohol varied from hours to weeks depending on the acid catalyst. Direct relation between the catalyst dissociation constant and the polymerization rate has not been observed because acid solubility in PFA resin also has an important influence on polymerization. PTLS was found to be the faster polymerization catalyst. Higher polymerization degree and residual weight were observed for the fastest catalysts, as PTLS and HCl acids. The specific surface area S_{BET} values of the MVC obtained were similar to those of nonporous carbon/silica surfaces, and varied from 1.4 to 7.4 m^2/g. Nitric acid catalyst corresponded to the highest micropore volume. The macroscopic porosity was

smaller for MVC produced with phosphoric and sulfuric acids that correspond to low polymerization rates. From the macroscopic porosity data, it was possible to compare relatively the MVC specific surface area (BET).

ACKNOWLEDGMENTS

REFERENCES

1. Jacobsen, A. J.; Mahoney, S.; Carter, W. B.; Nutt, S. *Carbon* **2011**, *49*, 1025.

2. Ju, M.; Zeng, C.; Wang, C.; Zhang, L. *Ind. Eng. Chem. Res.* **2014**, *53*, 3084.

3. Levendis, Y. A.; Flagan, R. C. *Carbon* **1989**, *27*, 265.

4. Men, X.-H.; Zhang, Z.-Z.; Song, H.-J.; Wang, K.; Jiang, W. *Appl. Surf. Sci.* **2008**, *254*, 2563.

5. Hu, C.; Sedghi, S.; Madani, S. H.; Silvestre-Albero, A.; Sakamoto, H.; Kwong, P.; Pendletonb, P.; Smernikf, R. J.; Rodríguez-Reinosoc, F.; Kanekog, K.; Biggsa, M. *J. Carbon* **2014**, *78*, 113.

6. Samuel, B. A.; Rajagopalan, C.; Foley, H.; Haque, M. A. *Thin Solid Films* **2010**, *519*, 91.

7. Jenkins, G. M.; Kawamura, K. Polymeric Carbons–Carbon Fiber, Glass and Char; Cambridge University Press: Cambridge, New York; **1976**; Chapter 1, p 1.

8. Chekanova, V. D.; Fialkov, A. S. *Russ. Chem. Rev.* **1971**, *40*, 413.

9. Zarzycki, J. Materials Science and Technology—A Comprehensive Treatment—Glasses and Amorphous Materials; Cahn, R. W.; Haasen, P.; Kramer, E. J., Eds.; Weinheim: New York, Basel, Cambridge, **1991**; Vol. *9*, Chapter 10, p 550.

10. Tseng, S. F.; Chen, M. F.; Hsiao, W. T.; Huang, C. Y.; Yang, C. H.; Chen, Y. S. *Opt. Laser. Eng.* **2014**, *57*, 58.

11. Olu, P. Y.; Barros, C. R.; Job, N.; Chatenet, M. *Electrocatalysis* **2014**, *5*, 288.

12. Simonet, J. *J Electrochem. Commun.* **2013**, *36*, 62.

13. Komarevskiy, N.; Shklover, V.; Braginsky, L.; Hafner, C.; Lawson, J. *Opt. Express.* **2012**, *20*, 14189.

14. Zhang, F.; Ilavsky, J.; Long, G. G.; Quintana, J. P. G.; Allen, A. J.; Jemian, P. R. *Metall. Mater. Trans. A.* **2010**, *41*, 1151.

15. Noda, T.; Inagaki, M.; Yamada, *J. Non-Cryst. Solids* **1969**, *1*, 285.

16. McKillip, W. J. *ACS Symp. Ser. 385*, **1989**, Chapter 29, 408.

17. Williams, D. L.; Dunlop, A. P. *Ind. Eng. Chem.* **1948**, *40*, 239.

18. Schmitt, C. R. *Polym. Plast. Technolo. Eng.* **1974**, *3*, 121.

19. Cheng, L.-T.; Tseng, W. J. *J Polym. Res.* **2010**, *17*, 391.

20. Hucke, E. E. U.S. Patent 3,859,421 (**1975**).

21. Oishi, S. S.; Rezende, M. C.; Origo, F. D.; Damião, A. J.; Botelho, E. C. *J. Appl. Polym. Sci.* **2013**, *128*, 1680.

22. Krishnan, T. A.; Chanda, M. *Die Angewandte Makromolekul. Chem.* **1975**, *43*, 145.

23. Brunauer, S.; Emmett, P.; Teller, E. *J. Am. Chem. Soc.* **1938**, *60*, 309.

24. Dubinin, M. M.; Astakhov, V. A.; Radushkevich, L. V. In Progress and Membrane Science; Cadenhead, D. A.; Danielli, J. F.; Rosenberg, M. D., Eds.; Academic Press: New York; **1975**; Vol. *9*, p 1.

25. Guthrie, J. P. *Can. J. Chem.* **1978**, *56*, 2342.

26. Goldstein, I.; Dreher, W. *Ind. Eng. Chem.* **1960**, *52*, 57.

27. Lide, D. R. CRC Handbook of Chemistry and Physics, 75th ed.; CRC Press: Boca Raton, FL; **1994**, p 6.

28. Munson, R. A. *J. Chem. Phys.* **1964**, *40*, 2044.

29. Gillespie, R. J.; White, R. F. M. *Trans. Faraday Soc.* **1958**, *54*, 1846.

30. Othmer, D. F. Encyclopedia of Chemical Technology, 3th ed.; New York, NY: Wiley; **1980**; Vol. *12*, p 985.

31. Guigo, N.; Mija, A.; Vincent, L.; Sbirrazzuoli, N. *Phys. Chem. Chem. Phys.* **2007**, *9*, 5359.

32. Barsberg, S.; Thygesen, L. G. *Vib. Spectrosc.* **2009**, *49*, 52.

33. Sing, K. S. W.; Everett, D. H.; Haul, R. A. W.; Moscou, L.; Pierotti, R. A.; Rouquerol, J.; Siemieniewska, T. *Pure Appl. Chem.* **1985**, *57*, 603.

34. Burket, C. L.; Rajagopalan, R.; Marencic, A. P.; Dronvajjala, K.; Foley, H. C. *Carbon* **2006**, *44*, 2957.

35. Fitzer, E.; Schaefer, W.; Yamada, S. *Carbon* **1969**, *7*, 643.

36. Carrott, P. J. M.; Sing, K. S. W.; Raistrick, J. H. *Colloid Surf.* **1986**, *21*, 9.

37. Carrott, P. J. M.; Roberts, R. A.; Sing, K. S. W. *Carbon* **1987**, *25*, 769.

38. Fukuyama, K.; Nishizawa, T.; Nishikawa, K. *Carbon* **2001**, *39*, 2017.

39. Edelson, L. H.; Glaeser, A. M. *Carbon* **1986**, *24*, 635.